The effect of tissue composition of the prostate on the dose calculation for ^{125}I brachytherapy

Takashi Hanada,[1,2,3] Atsunori Yorozu,[2] Toshio Ohashi,[1] Naoyuki Shigematsu,[1]
Kyoko Saito,[4] Koichi Maruyama[3,4]

[1] Department of Radiology, Keio University School of Medicine
[2] Department of Radiology, Tokyo Medical Center, National Hospital Organization
[3] Graduate School of Medical Sciences, Kitasato University
[4] School of Allied Health Sciences, Kitasato University

Objective: The purpose of the present study was to compare the effect of tissue composition of the prostate on dose calculation in the TG-43U1 formalism for ^{125}I brachytherapy of prostate carcinoma and to study how prostate medium differences lead to differences in dose distributions. Clinical significance of the results is also examined.

Methods: Geant4 Monte Carlo code was used to calculate dose distributions by simulation in four types of tissue compositions: water, average male soft tissue (AMST), skeletal muscle (SM), and the International Commission on Radiological Protection (ICRP) report No. 23 prostate tissue. The dosimetric parameters Λ and $g_L(r)$ for the prostate media were examined. The clinical dosimetry parameters of D_{100}, D_{90}, D_{80}, V_{200}, V_{150}, and V_{100} were evaluated by using the dosimetric parameters and the postplan CT images for 50 patients treated with permanent brachytherapy at the Tokyo Medical Center.

Results: The average differences of D_{90} (Gy) between water and prostate medium were 8.4 Gy $\pm$ 1.9 Gy for AMST, 0.7 Gy $\pm$ 0.5 Gy for SM, and 2.7 Gy $\pm$ 0.6 Gy for ICRP. The distribution of the differences of D_{90} between water and prostate medium was 5.2 $\pm$ 0.3% for AMST, 0.4 $\pm$ 0.3% for SM, and 1.7 $\pm$ 0.2% for ICRP. The dose volume histograms (DVHs) for SM and ICRP were close to that of water, while the DVH of AMST shifted to a lower dose.

Conclusions: The DVHs in water and prostate media showed small discrepancies. The TG-43U1-based calculation is acceptable to assumed a prostate medium comprised of homogeneous tissue that is equivalent to the weight of water and the use of water as a prostate medium is suitable for clinical dose calculations.

Key words: brachytherapy, iodine-125, Monte Carlo simulation, prostate carcinoma, dosimetry

Introduction

Permanent seed-implant treatment using ^{125}I radionuclide is currently a standard procedure for early-stage prostate carcinoma, and the method is now considered comparable to external-beam radiation therapy and prostatectomy.[1] As with external beam radiation therapy, permanent seed implant treatment of the prostate requires a dose-outcome correction, pointing out the importance of the planning process.[2] The positions and number of seeds are selected using the treatment planning system to achieve the best dose coverage of the prostate. The dose, calculated in accordance with the formalism established by the American Association of Physicists in Medicine Task Group No. 43 (AAPM TG-43), and the updated report (TG-43U1) is used in clinical practice to evaluate the two-dimensional dose deposited in water.[3,4]

The TG-43U1-based calculation assumes a prostate medium comprised of homogeneous tissue that is equivalent to the basic make up of water. However, the ways in which real prostate tissue composition differs from water may be important, because the absorption cross section due to the photoelectric effect of low-energy photons emitted from ^{125}I sources are proportional to the third to fourth power of the atomic number Z. Therefore, even small differences in effective atomic numbers of

water and the prostate lead to a difference in the cross sections of approximately more than 10%. It is possible that this difference causes a non-negligible effect in the real dose distribution, compared with that determined by the TG-43U1-based calculation.

Previous studies have suggested that only the accurate CT-based Monte Carlo technique, which takes into account the details of the implant, can accurately handle the effects of tissue heterogeneity.[5-7] However, in a real clinical situation, it is impossible to follow the procedure recommended by the physicians according to the findings of the studies described above because realistic prostate simulations are far too time consuming. While the TG-43U1-based calculation has the advantages of providing a fast, simple, and established method compared with the Monte Carlo simulation method, its most useful characteristic is the flexibility of dose-rate calculation during a real-time ultrasound-guided technique with intraoperative planning. Demonstrating the effect of prostate tissue composition on the TG-43U1-based calculation is therefore important for the accurate interpretation of the results of this method.[8]

The purpose of the present study was to compare the effect of the prostate media on the dose calculation using TG-43U1 clinical prostate implants with three different kinds of prostate media. The dosimetric parameters in the TG-43U1-based calculation, such as Λ and $g_L(r)$, were estimated in prostate medium using the Monte Carlo simulation code Geant4, since Λ and $g_L(r)$ are directly sensitive to the differences in the medium.[9] Subscript L denotes the use of the line source geometry function. The tissue composition effect can be studied by comparing the dose volume histogram (DVH) calculated in water with that calculated in a prostate medium using a revised TG-43U1-based calculation.

The institutional ethics committee of Tokyo Medical Center, National Hospital Organization and School of Allied Health Sciences, Kitasato University approved this retrospective study. Informed consent was waived, since it was not applicable due to the retrospective nature of the study.

Materials and Methods

Dose calculation formalism

The dose calculation formalism AAPM TG-43[3] and TG-43U1[4] was developed by the Interstitial Brachytherapy Collaborative Working Group to predict the dose distribution around cylindrically symmetric sources. According to this formalism, the dose rate $\dot{D}(r, \theta)$ in water, at a point expressed as (r, θ) in the polar coordinate

system relative to the geometric center of the line source, is given by the equation:

$$\dot{D}(r, \theta) = S_K \cdot \Lambda \cdot \frac{G_L(r, \theta)}{G_L(r_0, \theta_0)} \cdot g_L(r) \cdot F(r, \theta) \quad (1)$$

where r is the distance to the point of interest; r_0 denotes the reference distance, which is specified to be 1 cm; θ is the polar angle with respect to the longitudinal axis of the source; θ_0 is the reference angle that defines the source transverse plane and is specified to be $\pi/2$; S_K is the air-kerma strength; Λ is the dose-rate constant and corresponds to the dose rate at a distance of 1 cm on the transverse axis for a source with 1 unit of S_K; $G_L(r, \theta)$ is the geometry distribution given in cm^{-2} that accounts for spatial distribution of radioactive material; $F(r, \theta)$ is the anisotropy function that accounts for the angular dependence of photon absorption and scatter in the encapsulation and the medium; and $g_L(r)$ is the radial dose function that accounts for radial dependence of photon absorption and scatter in the medium along the transverse axis for the line-source model.

Two dosimetric parameters considered in the present study are given as follows.

$$\Lambda = \frac{\dot{D}(r_0, \theta_0)}{S_K} \quad (2)$$

$$g_L(r) = \frac{\dot{D}(r, \theta_0) \cdot G_L(r_0, \theta_0)}{\dot{D}(r_0, \theta_0) \cdot G_L(r, \theta_0)} \quad (3)$$

Detailed descriptions of the formalism can be found in the TG-43U1 report.[4]

Seed model

The Monte Carlo simulations were based on a complete 3-dimensional model of the 6711 source manufactured by General Electric Health Care. The model 6711 has been the most widely used source for permanent implantation since its introduction in 1983. This source consists of a 4.5 mm titanium capsule, 0.06 mm thick, with welded end caps. The capsule contains a cylinder silver rod core of 3.0 mm in length and 0.5 mm in diameter, coated with an Ag-halide of approximately 1 μm thickness onto which ^{125}I is absorbed. These source dimensions are the same as the ones used in the study by Williamson[10] and in the TG-43 update.[4] Figure 1 shows the geometry of the model 6711 source used in this Monte Carlo simulation.

Monte Carlo simulation

Simulations of particle transport in media were performed with the Geant4 (version 9.2) toolkit,[11] with a special

package of electromagnetic processes for photons and electrons for obtaining the dosimetric parameters. In recent studies, the Geant4 code was selected from several available Monte Carlo simulation codes for its combinatorial geometry capabilities, which allow an easy seed insertion into the 3D patient model.[6,7] Geant4 code has been used to validate the dosimetric parameters for ^{192}Ir and ^{137}Cs sources[12,13] and is well benchmarked, based upon the AAPM-ESTRO (European Society for Therapeutic Radiology and Oncology) recommendations.[14]

For calculation of the dosimetric parameters Λ and $g_L(r)$, the methodology proposed by Rodriguez et al. was

Figure 1. The geometry of the GE Health Care model 6711 source[1]

used.[15] The simulation geometry for calculating Λ, the air ring detector was located to surround the source, which was immersed in vacuum. An air ring detector is built with 1 cm height and 1 cm thickness and an inner and outer radius of 99.5 cm and 100.5 cm, respectively. In the air-kerma strength calculation, the characteristic x-rays from the titanium capsule were systematically suppressed to comply with the 1999 NIST standard. The simulation for $g_L(r)$, the source was located at the center of a water cylinder with dimensions sufficiently large to cover all of the simulation distances from the source. The cylinder was divided into a set of concentric rings with a width of 0.01 cm at distances to the source less than 0.2 cm, 0.05 cm at distances between 0.2 cm and 2 cm, 0.1 cm at distances between 2 cm and 5 cm, and a width of 0.5 cm at distances greater than 5 cm. The thickness of the cylinder was 0.01 cm at any distance.

The Geant4 code and the source modeling have to be validated through standard tests, including energy spectrum analysis, dose rate constant analysis, and radial dose function analysis. These data are acquired for the specific source used, and compared with published values.

Density and elemental composition of prostate medium
To evaluate the effect of tissue composition on the dose distribution in the prostate for the ^{125}I brachytherapy, Geant4 code was used to simulate four different media. In the first calculation, prostate medium is made of pure water, which is the conceptual basis of TG-43U1. In the second calculation, prostate medium is made of average male soft tissue (AMST) as defined in the ICRU report 44.[16] In the third calculation, prostate medium is made of ICRU report 44 skeletal muscle (SM).[16] In the last calculation, prostate medium is made of ICRP report 23 prostate tissue (ICRP).[17] Table 1 shows the elemental compositions and densities of the prostate media used for this study. The effective atomic number of the prostate
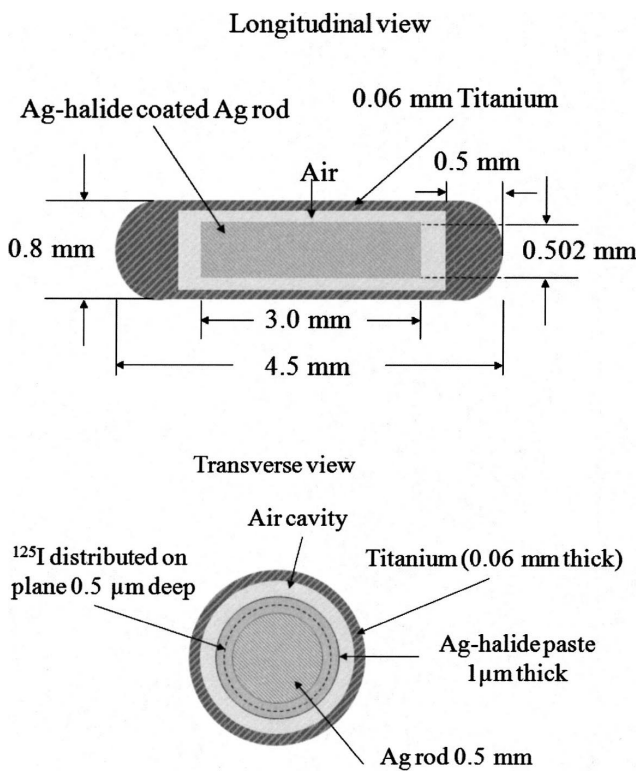
Table 1. Density and composition of prostate media obtained from the literature[15,16]

Density (g-cm⁻³)	Water						1.000						
	AMST						1.030						
	SM						1.050						
	ICRP						1.045						

		H	C	N	O	Na	P	S	Cl	K	Ca	Zn	Mg
Weight (%)	Water	11.1	0.0	0.0	88.9	0.0	0.0	0.0	0.0	0.0	0.0	0.0	0.0
	AMST	10.5	25.6	2.7	60.2	0.1	0.2	0.3	0.2	0.2	0.0	0.0	0.0
	SM	10.2	14.3	3.4	71.0	0.1	0.2	0.3	0.1	0.4	0.0	0.0	0.0
	ICRP	9.76	9.11	2.47	78.1	0.21	0.1	0.0	0.0	0.2	0.023	0.008	0.019

medium developed by AMST was 7.45, while it was 7.70 for SM and 7.66 for ICRP.

In this article, the dosimetric parameters Λ and $g_L(r)$ calculated in water are expressed as Λ_{water} and $g_L(r)_{water}$, and those in a prostate medium (pm) are expressed as Λ_{pm} and $g_L(r)_{pm}$ (subscript pm represents one of the prostate medium such as AMST, SM and ICRP).

Clinical dosimetry parameters

This retrospective study focused on post-plan dosimetry calculations for the DVH, compared among a subgroup of 50 randomly selected patients from 202 patients. Thirty patients were treated with seed implantation alone to deliver a minimum dose of 160 Gy. The remaining 20 patients received combined therapy of a minimum dose of 100-110 Gy for seed implantation and a boosted dose of 45 Gy for external beam radiotherapy. These patients had been treated with permanent brachytherapy between January 2008 and December 2008 at the Tokyo Medical Center. Table 2 details the characteristics of patients of this subgroup. For post-plan dosimetry, a CT scan was performed on the patient approximately 4 weeks after implantation, with a slice thickness of 3.0 mm. The prostate was contoured by the physician on the CT datasets and detailed dose information, including clinical dosimetry parameters, was obtained with a dose calculation engine. For the present study, we used the clinical dose calculation engine from the VariSeed system (Varian). The dose calculation algorithm of the engine manipulates dosimetric parameters, such as Λ and $g_L(r)$, which are derived from the TG-43U1-based calculation that is expressed in equation (1).

Clinical dosimetry parameters such as D_{100}, D_{90}, D_{80}, V_{200}, V_{150}, and V_{100} in respective media were obtained using the above method, installing the calculated values of Λ_{pm} and $g_L(r)_{pm}$ into the VariSeed source file, and these were compared for each patient. Here, D_X is the minimal dose deposited in X% of the medium volume, and V_X is the medium volume covered by X% of the prescription dose.

In this study, when two media are compared, results are given in terms of relative differences. The relative differences of D_X values between water ($D_{X, water}$) and other prostate medium ($D_{X, pm}$) are given as follows.

$$\Delta D_X(Gy) = D_{X, water} - D_{X, pm} \tag{4}$$

$$\Delta D_X(\%) = \frac{D_{X, water} - D_{X, pm}}{D_{X, water}} \tag{5}$$

For V_X values are given in percentages, the relative difference is given as follows.

$$\Delta V_X(\%) = V_{X, water} - V_{X, pm} \tag{6}$$

Results and Discussion

Validation of the Monte Carlo simulation

We applied the method to obtain the energy spectrum, dose-rate constant, and radial dose function in water to assess the accuracy of the present Monte Carlo simulation method with Geant4. We compared these results with those of TG-43U1 as well as with some published data.

The photon energy spectrum of ^{125}I used in this study was obtained from the NuDat 2 database.[18] A comparison is drawn between the photon energy spectrum obtained using Geant4 and other spectra found in literature (Table 3). The published spectra were either measured experimentally[19,20] or calculated using Monte Carlo simulation.[6,21] The six peaks come from different processes. The three lower energy peaks are fluorescence peaks due to the titanium shell and the silver rod. The three more energetic peaks are directly due to the ^{125}I radionuclide decay (electron capture decay produces 27.4 keV Te K_α and 31.0 keV Te K_β gammas, while gamma ray transition produces 35.5 keV gammas). It should be noted that the spectra have been normalized to 1.0 at the 27.4 keV peak. The difference between the results for the two Monte Carlo Geant4 codes was less than 1.0% of the major peak intensity for any of the five other peaks.

The dose-rate constant and the radial dose function, obtained in a similar way by the present authors, were compared with TG-43U1 values and the results of Dolan

Table 2. Characteristics of 50 patients used for the analysis of the DVH

	Median	Standard Deviation	Maximum	Minimum
Age	66	7	79	46
Prostate Volume (cc)	30.61	6.76	52.50	17.77
Number of Seeds	74	13	104	45
Gleason Score	6	1	9	5

et al.[22] and Kirov et al.,[23] and these proved to be in good agreement.[8] Accordingly, we believe that our method exhibited sufficient reliability and validity to carry out calculations of the dosimetric parameters in the prostate media.

Comparison of the dosimetric parameters
The calculated dosimetric parameters in water, Λ_{water} and $g_L(r)_{water}$ were compared to the calculated values in each prostate medium, Λ_{pm} and $g_L(r)_{pm}$.

The dose rate constants water Λ_{water}, calculated in our study, was 0.964 cGyh^{-1}U^{-1} and for prostate medium Λ_{pm} were 0.905 cGyh^{-1}U^{-1} for AMST, 0.971 cGyh^{-1}U^{-1} for SM, and 0.956 cGyh^{-1}U^{-1} for ICRP. The relative differences between the Λ_{water} value and the Λ_{pm} values were 6.1% for AMST, 0.7% for SM, and 0.8% for ICRP. The Λ_{pm} of AMST was clearly lower than Λ_{water}. The other two Λ_{pm} values, SM and ICRP, were slightly affected by medium composition.

The results of the radial dose function in prostate medium $g_L(r)_{pm}$ at distances of $0.1 < r < 10$ cm are plotted in Figure 2 and the differences between $g_L(r)_{water}$ and $g_L(r)_{pm}$ are plotted in Figure 3. The radial dose function $g_L(r)$ exhibits a prominent difference in the region over 2 cm, and this difference is maintained within 3.3% for all prostate medium in the region close to the source.

Table 3. Comparison between the photon energy spectrum calculated using Geant4 and other published spectra

Energy (keV)	Relative peak intensity					Carrier-this work
	Ling	Kubo	Bohm	Carrier	This work	
4.5	-	0.0089	0.0081	0.0078	0.0074	0.0004
22.1	0.25	0.263	0.240	0.240	0.235	0.005
25.2	0.07	0.075	0.065	0.0625	0.0620	0.0005
27.4	1.0	1.0	1.0	1.0	1.0	-
31.0	0.25	0.228	0.235	0.231	0.224	0.007
35.5	0.06	0.048	0.07	0.068	0.064	0.004

Data are presented relative to the major peak intensity. Bohm et al.[20] used MCNP and Carrier used Geant4[5] to calculate their spectra, while Ling et al.[18] and Kubo[19] performed experimental measurements.
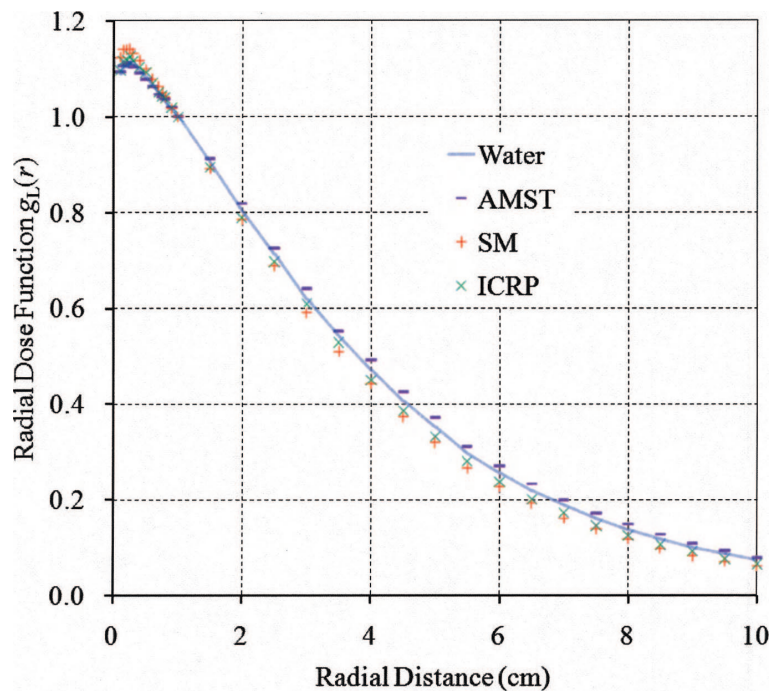

Figure 2. Radial dose functions in water and three prostate media

Clinical significance

A list of clinical dosimetry parameters, such as D_{100}, D_{90}, D_{80}, V_{200}, V_{150}, and V_{100}, are presented in Table 4 and the relative differences are presented in Table 5, in which values in water and each prostate medium are compared. For clinical dosimetry parameters in Table 4, the mean values are given as well as the difference between the prostate medium in Table 5. Regarding the prostate media, we observed a systematic decrease in the deposited dose of D_{100}, D_{90}, and D_{80} when compared with water. For example, the average differences of D_{90} (Gy) between water and prostate medium made of AMST was 8.4 Gy with a standard deviation of 1.9 Gy. The same comparison for the prostate media made of SM and ICRP leads to 0.7 Gy with a standard deviation of 0.5 Gy and 2.7 Gy decreases with a standard deviation of 0.6 Gy for D_{90}.

The distribution of the differences of D_{90} between water and prostate media is presented in Figure 4 and shows a spread of 5.2 ± 0.3% for AMST, 0.4 ± 0.3% for SM, and 1.7 ± 0.2% for ICRP.

Figure 5 shows the cumulative DVH in water and in each prostate medium. The prostate medium DVHs for SM and ICRP are very close to that of water, while the DVH of AMST is clearly shifted to a lower dose. Water is the medium with the lowest density, but with the highest oxygen content, which is the dominant element with regards to photoelectric absorption. AMST, SM, and ICRP have similar densities, but different oxygen contents. Water and SM and ICRP prostate media produced much closer DVHs although water has a higher oxygen content in comparison with SM. The lower oxygen content in SM is compensated by its higher density
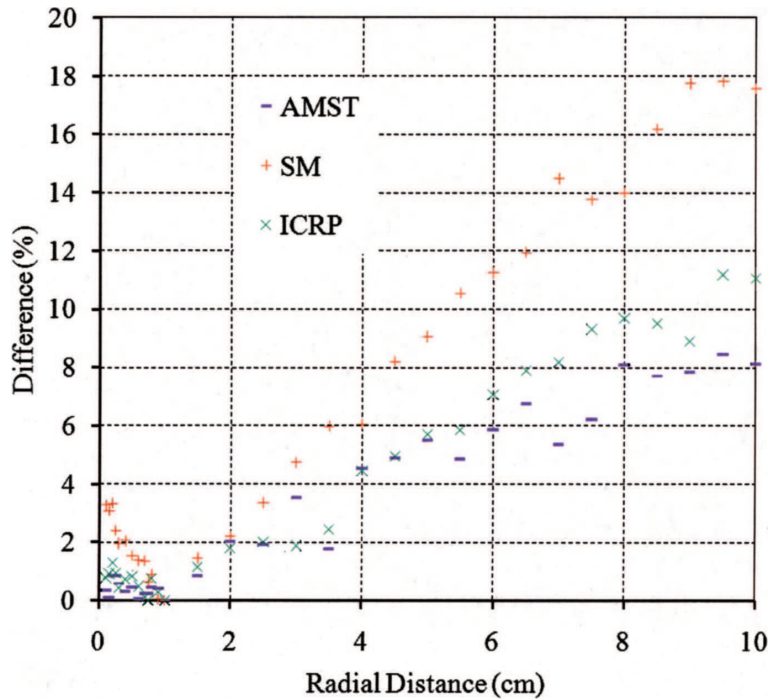

Figure 3. Differences in radial dose functions for three prostate media compared with water

Table 4. Summary of clinical dosimetry parameters for the DVH

Parameter	Water	AMST	SM	ICRP
D_{100} (Gy)	105	100	104	103
D_{90} (Gy)	161	152	160	158
D_{80} (Gy)	175	166	174	172
V_{200} (%)	28	23	28	27
V_{150} (%)	62	54	62	60
V_{100} (%)	98	97	98	98

Table 5. The relative differences between prostate media and water as defined in eq. 4 and eq. 6

Parameter	AMST	SM	ICRP
D_{100} (Gy)	4.9 ± 0.2	1.1 ± 0.4	1.9 ± 0.2
D_{90} (Gy)	5.2 ± 0.2	0.4 ± 0.3	1.7 ± 0.2
D_{80} (Gy)	5.3 ± 0.1	0.3 ± 0.3	1.6 ± 0.1
V_{200} (%)	4.7 ± 1.5	-0.7 ± 0.2	0.9 ± 0.3
V_{150} (%)	8.1 ± 1.5	-0.1 ± 0.4	2.0 ± 0.5
V_{100} (%)	1.4 ± 1.5	0.2 ± 0.3	0.4 ± 0.5

in comparison with water. AMST leads to less energy-deposition in the prostate tissue, therefore it lowers D_{100}, D_{90}, and D_{80} in comparison with water. The slightly higher density of AMST does not fully compensate for its lower oxygen content in comparison with water.

The V_{100} value stayed almost constant, with a maximum difference of 1.4% for AMST, indicating that

volume coverage was equivalent in all prostate media.

The low energy range of photons emitted from ^{125}I, where the photoelectric effect is the dominant absorption process, is one of the factors that causes differences in absorption and scattering properties between water and other tissue media. The average photon energy emitted from ^{125}I is approximately 28 keV. For example, at an
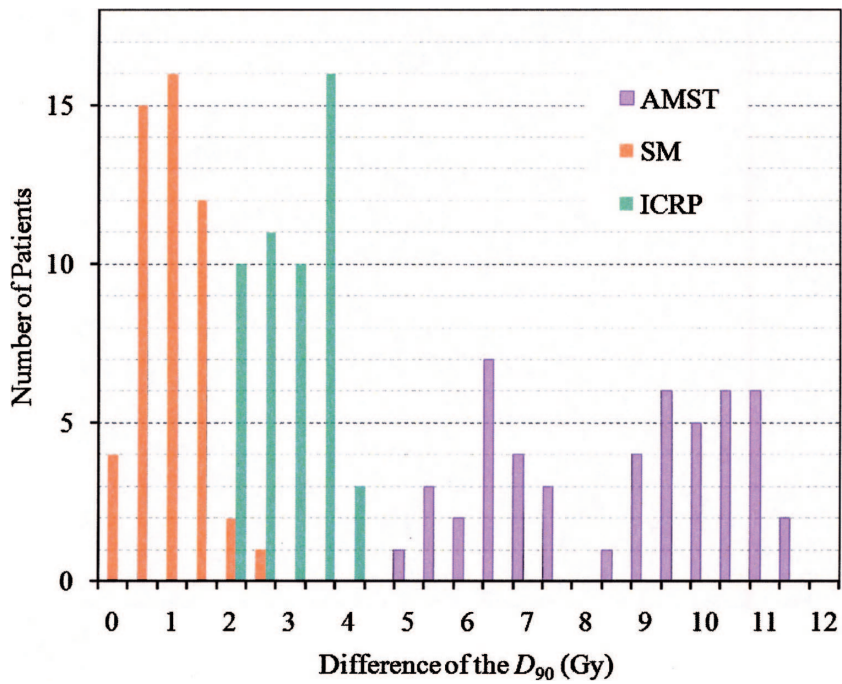

Figure 4. Distribution of differences of D_{90} between water and three prostate media
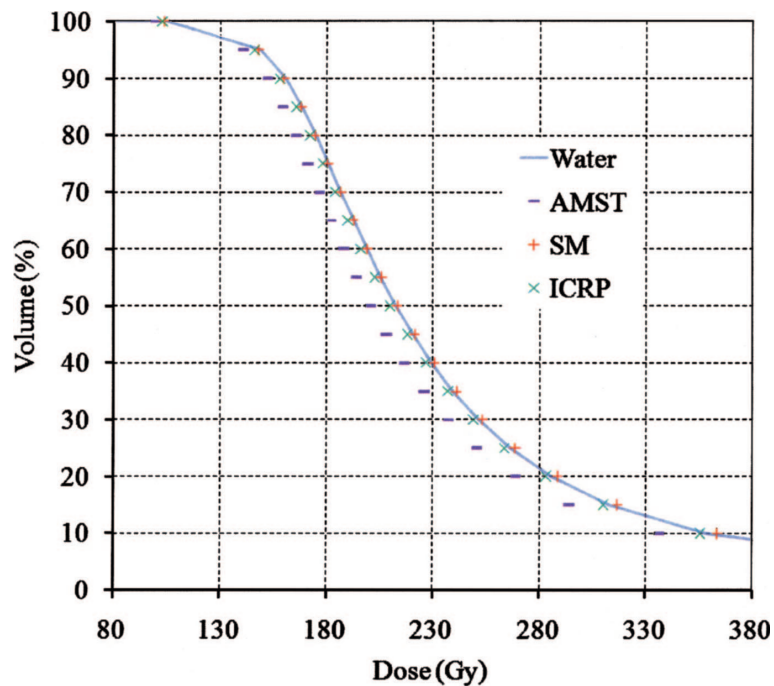

Figure 5. Dose volume histograms calculated in water (solid curve), AMST (-), SM (+), and ICRP ($\times$)

energy of 30 keV, the mass energy absorption coefficient for water $(\mu_{en}/\rho)_{water}$ is 0.1557 cm^3/g and for soft tissue $(\mu_{en}/\rho)_{soft}$ is 0.1616 cm^3/g. In the case of adipose tissue, $(\mu_{en}/\rho)_{adipose}$ is 0.09495 cm^3/g; that is, absorption and scattering properties between water and adipose tissue exhibit a difference in (μ_{en}/ρ) of approximately 40%.

Several studies of the value of D_{90} have been carried out, in addition to our finding of a 0.4 % to 5.2 % difference in D_{90} between water and other prostate media. In a previous study, Demarco et al.[24] used Monte Carlo simulations to evaluate tissue heterogeneity effects and compared the effects with results obtained with TG-43-based calculations. To this end, the researchers simulated ^{125}I prostate implants merged in CT-based heterogeneous phantoms. The use of a CT-based heterogeneous phantom, compared with a pure water phantom, resulted in a 5.6% decrease in the volume of tissue irradiated by a described isodose line of 144 Gy. A study by Chibani et al.[5] reported a decrease of 2.4%, comparing water and average male soft tissue using a Monte Carlo simulation technique. Chibani et al.[5] also showed a clearly left-shifted DVH of prostate when prostate tissue is assumed to be made of average male soft tissue, but not when made of skeletal muscle. Carrier et al.[6] reported the difference between Monte Carlo simulations in water and Monte Carlo simulations in prostate tissue made of ICRP and published values of between 4.4% and 4.8% for the 26 cm^3 and 59 cm^3 prostate sizes, respectively, on D_{90}. Carrier et al.[7] also reported an average 2.6% decrease in systematic effects using a realistic Monte Carlo calculation from patient data that considered more than 200 available tissue combinations of variable densities and elemental compositions. We previously reported the evaluation of the D_{90} calculated by the prostate medium determined from the CT images of 149 patients.[8] The results show a systematic dose overestimation of 2.8 $\pm$ 0.7 Gy in water, whereas the distribution of the differences can be seen with a spread of 1.8 $\pm$ 0.3% compared to that in prostate medium.

Interobserver differences in post-plan dosimetry are well known as a significant problem because of the unclear boundaries between the prostate tissue and its adjacent organs.[25] In addition, remarkable interobserver differences occur in D_{90}. Aoki et al. reported that variance in D_{90} caused by interobserver differences in postplan dosimetry is more than $\pm$ 10% from the reference D_{90}.[26] The current results showed a small discrepancy of 0.4% to 5.2%, between water and other prostate media, compared with the variance in the problem of interobserver differences. As long as the TG-43U1-based

calculation is used in clinical treatment planning, the prescription dose should not be changed by such a small discrepancy. Therefore, the TG-43U1-based calculation used in the treatment planning is adequate for a prostate medium comprised of homogeneous tissue that is equivalent to water. Our results are valuable to confirm the differences in the dose calculation caused by changes in tissue composition.

The TG-43U1-based calculation is widely used in treatment planning as the established method for real-time ultrasound-guided techniques, because of its advantages in speed, reliability, and simplicity. In the present study, the dosimetric parameters of the TG-43U1-based calculation in homogeneous prostate media, determined from AMST, SM, and ICRP, were calculated and compared with those in water. A comparison of D_{90} values shows a systematic dose underestimation of 5.2 $\pm$ 0.3% in AMST, 0.4 $\pm$ 0.3% in SM, and 1.7 $\pm$ 0.2% in ICRP, compared with that in water. Our results revealed that only minor discrepancies in the DVHs in water and other prostate media are comparable to the dose error variance caused by interobserver differences. The TG-43U1-based calculation is acceptable to a prostate medium comprised of homogeneous tissue equivalent to water in clinical intraoperative dose calculation.

Acknowledgments

References

1. Stokes SH, Real JD, Adams PW, et al. Transperineal ultrasound-guided radioactive seed implantation for organ-confined carcinoma of the prostate. *Int J Radiat Oncol Biol Phys* 1997; 37: 337-41.

2. Stock RG, Stone NN, Tabert A, et al. A dose-response study for I-125 prostate implants. *Int J Radiat Oncol Biol Phys* 1998; 41: 101-8.

3. Nath R, Anderson LL, Luxton G, et al. Dosimetry of interstitial brachytherapy sources: recommendations of the AAPM Radiation Therapy Committee Task Group No. 43. American Association of Physicists in Medicine. *Med Phys* 1995; 22: 209-34.

4. Rivard MJ, Coursey BM, DeWerd LA, et al. Update of AAPM Task Group No. 43 Report: A revised AAPM protocol for brachytherapy dose calculations. *Med Phys* 2004; 31: 633-74.

5. Chibani O, Williamson JF, Todor D. Dosimetric effects of seed anisotropy and interseed attenuation for ^{103}Pd and ^{125}I prostate implants. *Med Phys* 2005; 32: 2557-66.

6. Carrier JF, Beaulieu L, Therriault-Proulx F, et al. Impact of interseed attenuation and tissue composition for permanent prostate implants. *Med Phys* 2006; 33: 595-604.

7. Carrier JF, D'Amours M, Verhaegen F, et al. Postimplant dosimetry using a Monte Carlo dose calculation engine: a new clinical standard. *Int J Radiat Oncol Biol Phys* 2007; 68: 1190-8.

8. Hanada T, Yorozu A, Ohashi T, et al. Evaluation of the dosimetric parameters for ^{125}I brachytherapy determined in prostate medium using CT images. *J Radiat Res* 2010; 51: 553-61.

9. Yu Y, Anderson LL, Li Z, et al. Permanent prostate seed implant brachytherapy: report of the American Association of Physicists in Medicine Task Group No. 64. *Med Phys* 1999; 26: 2054-76.

10. Williamson JF. Monte Carlo evaluation of specific dose constants in water for ^{125}I seeds. *Med Phys* 1988; 15: 686-94.

11. Agostinelli S, Allison J, Amako K, et al. GEANT4--a simulation toolkit. *Nucl Instrum Methods Phys Res A* 2003; 506: 250-303.

12. Granero D, Pérez-Calatayud J, Ballester F. Monte Carlo study of the dose rate distributions for the Ir2.A85-2 and Ir2.A85-1 Ir-192 afterloading sources. *Med Phys* 2008; 35: 1280-7.

13. Pérez-Calatayud J, Granero D, Casal E, et al. Monte Carlo and experimental derivation of TG43 dosimetric parameters for CSM-type Cs-137 sources. *Med Phys* 2005; 32: 28-36.

14. Li Z, Das RK, DeWerd LA, et al. Dosimetric prerequisites for routine clinical use of photon emitting brachytherapy sources with average energy higher than 50 kev. *Med Phys* 2007; 34: 37-40.

15. Rodríguez EA, Alcón EP, Rodriguez ML, et al. Dosimetric parameters estimation using PENELOPE Monte-Carlo simulation code: Model 6711 a ^{125}I brachytherapy seed. *Appl Radiat Isot* 2005; 63: 41-8.

16. ICRU (International Commission on Radiation Units and Measurements) Report 44. Tissue substitutes in radiation dosimetry and measurements. Bethesda, MD, USA, *ICRU* 1989.

17. Snyder WS, Cook MJ, Nasset ES, et al. Report of the task group on reference man. Technical Report No. 23. *ICRP (International Commission on Radiological Protection)* 1974.

18. National Nuclear Data Center, NuDat 2.5 Database, Available at: http://www.nndc.bnl.gov/nudat2/. Accessed April 8, 2009.

19. Ling CC, Yorke ED, Spiro IJ, et al. Physical dosimetry of 125I seeds of a new design for interstitial implant. *Int J Radiat Oncol Biol Phys* 1983; 9: 1747-52.

20. Kubo H. Exposure contribution from Ti K x rays produced in the titanium capsule of the clinical I-125 seed. *Med Phys* 1985; 12: 215-20.

21. Bohm TD, DeLuca PM, DeWerd LA. Brachytherapy dosimetry of ^{125}I and ^{103}Pd sources using an updated cross section library for the MCNP Monte Carlo transport code. *Med Phys* 2003; 30: 701-11.

22. Dolan J, Lia Z, Williamson JF. Monte Carlo and experimental dosimetry of an ^{125}I brachytherapy seed. *Med Phys* 2006; 33: 4675-84.

23. Kirov AS and Williamson JF. Monte Carlo-aided dosimetry of the Source Tech Medical Model STM1251 I-125 interstitial brachytherapy source. *Med Phys* 2001; 28: 764-72.

24. Demarco JJ, Smathers JB, Burnison CM, et al. CT-based dosimetry calculations for ^{125}I prostate implants. *Int J Radiat Oncol Biol Phys* 1999; 45: 1347-53.

25. Merrick GS, Butler WM, Dorsey AT, et al. The dependence of prostate postimplant dosimetric quality on CT volume determination. *Int J Radiat Oncol Biol Phys* 1999; 44: 1111-7.

26. Aoki M, Yorozu A, Dokiya T. Evaluation of interobserver differences in postimplant dosimetry following prostate brachytherapy and the efficacy of CT/MRI fusion imaging. *Jpn J Radiol* 2009; 27: 342-7.